College of Saint Benedict and Saint John's University

DigitalCommons@CSB/SJU

Physics Student Work

Physics

7-8-2019

Magnetohydrodynamic Salt Water Drive

Noah Schmelzer
College of Saint Benedict/Saint John's University, NJSCHMELZER@CSBSJU.EDU

Recommended Citation

Magnetohydrodynamic Salt Water Drive

by

Noah Schmelzer

May 3, 2019

St. John's University

Contents

Abstract

Magnetohydrodynamics (MHD) is the behavior of conducting fluids in electric and magnetic fields. Plasmas, liquid metals, and water are all examples of a conducting fluid with magnetic properties. Much of MHD is fluid-flow and the effects of electromagnetic fields on them, but propulsion is also a possibility. A magnetohydrodynamic salt water propulsion system was constructed to observe the effects of salinity on resistivity, and then on the overall efficiency of the drive. Salinity of water and corresponding resistivity was altered to optimize fluid velocity. The apparatus used was a rectangular tube with permanent magnets perpendicular to aluminum electrodes. The fluid acts as a conductor for the Lorentz force, effectively creating an underwater drive without moving parts. In a static no-flow setup, a pressure differential on the order of 10 Pascals was measured. In steady-state free flow, fluid flow of approximately 1 meter per second was observed.

Introduction

Background

I first heard of magnetohydrodynamics, the behavior of conducting fluids in electric and magnetic fields, in Tom Clancy's 1984 novel *The Hunt for the Red October* and later Paramount Pictures film of the same name. In the story, the experimental Soviet caterpillar drive is described as a cutting-edge silent propulsion system. The stealth benefits of a propulsion system without moving parts touted by the novel was analyzed in 1991 with the Japanese ship Yamato-1 (Sasakawa). While a few creative liberties were taken in *The Hunt for the Red October*, a similar drive is possible to construct. Water, however, is not the only magnetohydrodynamic fluid;

plasmas (such as between the Sun and Earth, the most studied MHD fluid), liquid metals, and air are all examples of a conducting fluid with magnetic properties. At the beginning of this project, I was interested in the Lorentz force as propulsion, and initially picked plasma as my fluid for a magnetohydrodynamic drive. The extremely high voltages required as well as the complex fluid-flow equations were toned down by a safer and simpler medium: salt water. My goal then changed to modelling, building, and optimizing a water drive.

I began the project by researching published expeditions into water drives and found reference to the Japanese experimental ship named Yamato-1. I read here that maximizing conductivity is central to higher velocities and that salt water is a much better conductor than pure water, prompting my interest in resistivity versus water salinity. An established proof-of-concept in the Yamato-1 showed me that MHD propulsion was possible, even though it was deemed commercially implausible. I then moved onto making my own drive.

The effect that drives these MHD drives is known as the Lorentz force. A current moving perpendicular to a magnetic field produces a force on the charge carrier perpendicular to both the magnetic field and the current, allowing for propulsion to occur. (Figure 1).
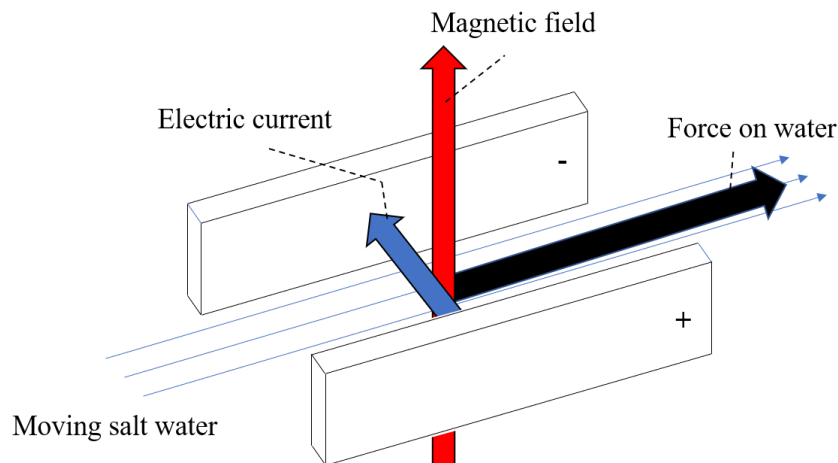

Figure 1: Diagram demonstrating the Lorentz Force.

I started by mocking up a small-scale prototype with small, rectangular magnets, two aluminum electrodes perpendicular to these magnets with two six-volt batteries, and a square

tube made from acrylic (Figure 2). With this setup, I was able to see a weak flow of roughly one centimeter per second. I then moved to scale up the magnetic field and to have a more regulated. voltage source. Using the same acrylic tube with new electrodes and stronger magnets, I had my final prototype.

Figure 2: Left, small scale prototype; right, final prototype. Note difference in magnet

size (1 cm x 0.25 cm x 6 cm versus 7.5 cm x 2 cm x 15 cm).

Research Methods

Each research method was designed to investigate a different characteristic of the drive as salinity was varied. As an optimization parameter, electrical resistance of water varies with its salinity, and so each experiment used 4 percent (approximately seawater salinity), 7 percent, and 10 percent salinity by mass to investigate the influence of lower resistivity on the drive (Table 1).

Salinity by mass (%)	Resistivity at standard temperature and pressure ($\Omega \cdot m$)
0.0	-
1.0	0.564
2.5	0.242
5.0	0.131
7.5	0.093
10.0	0.074
12.5	0.062

Table 1: Table of salinities and resistivities (Crain).

My research methods took four forms: computer modelling of a simplified drive, examination of electrical power in versus mechanical power out, measurement of a pressure differential, and calculation of water velocity. In the computer model, a theoretical force per unit volume differential equation was solved in one dimension to approximate the fluid velocity in the steady-state case. Wolfram Mathematica was used for this, due to familiarity with it from previous labs. This gave a reference point for what was to be expected from further experiments.

By using a simple circuit consisting of a DC power source, an ammeter, and a voltmeter, electrical power to the resistor (the salt water between the electrodes) could be measured (Figure 3). Two measurements were taken for various salinities, one as current versus voltage without a magnetic field present and the other as current versus voltage with a magnetic field present. By subtracting the electrical power in at the same voltages from the two measurements, the mechanical power could be calculated.
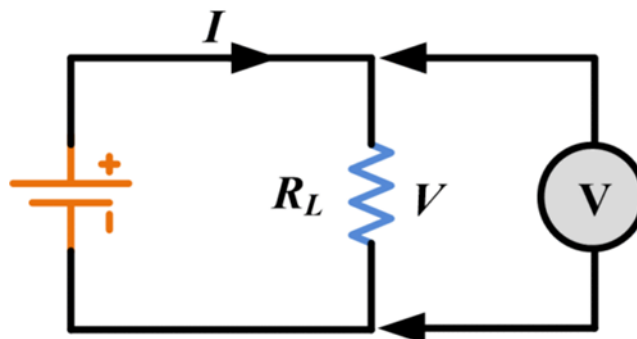

Figure 3: Diagram of electrical power circuit

The next experimental setup was to find the force the drive produced. A static, no-flow scenario was desirable for this. Although it would not produce power while in a no-flow state (no displacement once in equilibrium), the drive's force could be extrapolated from the difference in water level height in an elbow joint. A specially created elbow joint was sealed to the end of the acrylic tube underwater, which was set to maximum electrical power in. The resulting displacement was matched to a "ballpark" estimate for the force, giving a point of reference for differing salinities.

The final research method was simply to observe the fluid velocities at maximum electrical power in. Drops of ink were entered from a syringe into the front of the drive and were video recorded crossing a ruler. By analyzing the distance traveled over the time taken, the velocity could be found at different salinities.

Theory

Computer Model

Force per water molecule requires immense computing power to model at a macro scale. Instead, I looked at the force on a piece (small volume cube) of fluid and how it moved from there. The following derivations stem from Navier-Stokes fluid-flow equations and electricity and magnetism under ideal magnetohydrodynamic settings. A discussion of these assumptions follows at the end of the subsection. The result of the derivation is a three-dimensional differential equation that could be approximated to one dimension in a Wolfram Mathematica model.
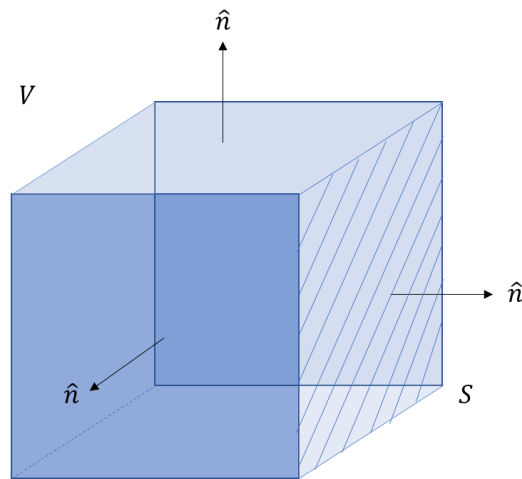

Figure 4: Cube bounded by surface.

To begin, take a cube (Figure 4) with volume V bounded by a surface S. Then the total mass equals

$$M = \int_V \rho \, dV \tag{1}$$

with ρ as water density. Taking the time derivative of both sides, we get the change in mass with time.

$$\frac{dM}{dt} = \int_V \frac{\partial \rho}{\partial t} \, dV \qquad (2)$$

Taking $d\vec{s} = \hat{n} \, ds$, the mass through some surface is $\rho \vec{v} \cdot d\vec{s}$, where $\vec{v}$ is the velocity of the fluid. Then,

$$\int_V \frac{\partial \rho}{\partial t} \, dV = -\oint_S \rho \vec{v} \cdot d\vec{s} \qquad (3)$$

by Gauss' Theorem, (3) becomes

$$\int_V \left(\frac{\partial \rho}{\partial t} + \nabla \cdot (\rho \vec{v}) \right) dV = 0 \qquad (4)$$

If we say that water is incompressible (a good approximation), then $\frac{\partial \rho}{\partial t} = 0$. Equation (4) tells us

$$\nabla \cdot (\rho \vec{v}) = 0 \qquad (5)$$

giving us a continuity equation: mass is not created or destroyed in this process. Taking a force per unit volume acting on a piece of fluid, we get

$$\vec{F} = \rho \frac{d\vec{v}}{dt} \qquad (6)$$

Opposing this force per unit volume, we have the force of the flow-induced electric field

$$\vec{F_I} = \frac{q}{V} \vec{E_I} \qquad (7)$$

$$\vec{E_I} = B \vec{v} \qquad (8)$$

where q is the charge on an ion and V is the volume of the tube. This term describes the top limit for the fluid velocity and will contribute to the later derivation of the drive's efficiency.

The main force of this system is the Lorentz force (ignoring $\vec{F}_{electric} = q\vec{E}$ term here as charges are assumed to be moving)

$$\vec{F_L} = \vec{J} \times \vec{B} \tag{9}$$

where $\vec{J} = \rho_c \vec{v}$ is the current density vector and $\vec{B}$ is the magnetic field vector, with $\rho_c = \frac{q}{V}$ as the charge density. Another force per unit volume comes from the bulk motion or advection of the velocity field from fluid flow:

$$\vec{F_a} = \rho(\nabla \cdot \vec{v})\vec{v} \tag{10}$$

This can be thought of as the gradient in velocity affecting other fluid flow through dissipation. Putting equations (6) through (9) together with Newton's Second Law, we get our main equation

$$\rho\frac{d\vec{v}}{dt} + \rho(\nabla \cdot \vec{v})\vec{v} = \vec{J} \times \vec{B} - \rho_c B\vec{v} \tag{11}$$

This tells us the force per unit volume plus the bulk motion of the fluid is equal to the magnitude of the Lorentz force minus the velocity dependent induced E-field force. This does not consider eddy currents, fluid friction on the tube's walls, gravity, or any viscosity forces. For modelling purposes, the spatial derivatives were taken along the long dimension of the tube, the $\hat{z}$ direction, with the final velocity as a function of time and displacement in the $\hat{z}$ direction. Initial conditions were taken as the fluid is initially at rest with respect to time and with respect to $z = 0$ displacement.

These equations assume ideal magnetohydrodynamics. Strong intermolecular collisions must occur between fluid particles, resistivities need to be small, and the modelling is not taking

place on atom-sized scales. This final assumption allows for bulk motion of the fluid to be approximated and made much simpler.

Pressure Differential

The force required to lift a fluid from an initial height h_0 to a final height h_f is:

$$\vec{F} = (h_f - h_0)\, A_l\, \rho\, g \tag{12}$$

Where A_l is the area of fluid lifted, ρ is the water density, and g is the force of gravity. If (12) is divided by area A, we get a force per unit area or pressure. By varying water salinity, the force should change proportionally.

Electrical Power vs. Mechanical Power

The current present in the Lorentz force uses salt ions in the water as a conductor, meaning the dimensions of the tube will affect the amount of resistive material the current must flow through (Figure 5). Therefore, the more salt present (or higher salinity) the lower electrical resistance there will be. The resistance can be calculated using the resistance formula

$$R = \frac{\rho_s \ell}{h\, w} \tag{13}$$

with ρ_s the resistivity of salt water, ℓ the length of the electrodes, h the height of the electrodes, and w the electrode separation. The "no-load" electric power $P_{no\ load}$, (no magnetic field
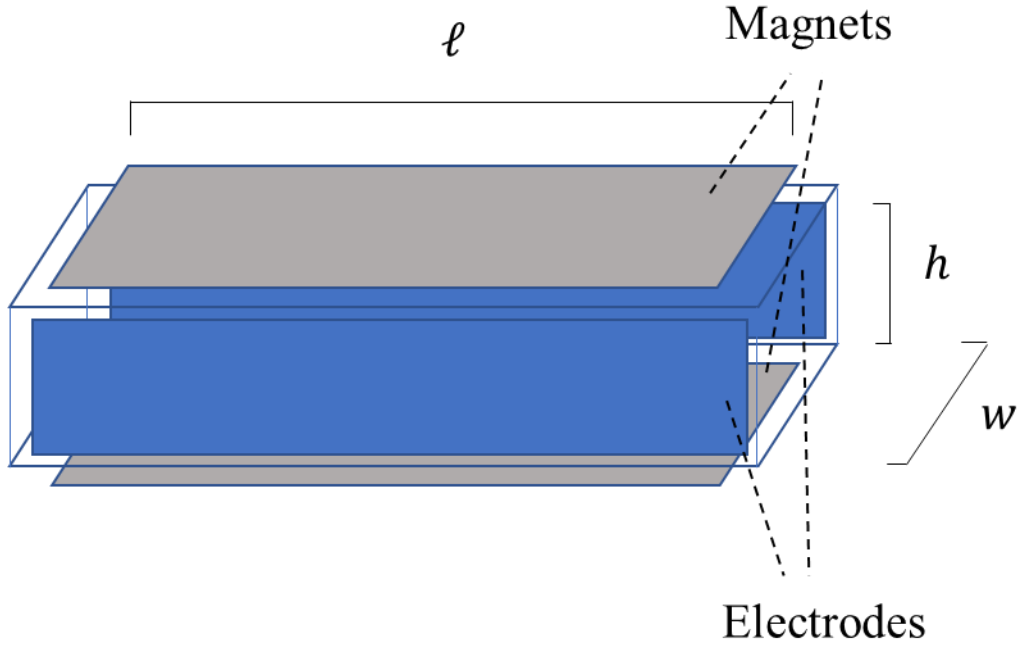
Figure 5: Tube dimensions diagram.

present) can be subtracted from the loaded electrical power, P_{load}, to find the mechanical power, P_{mech}:

$$P_{elec} = V\,I \tag{14}$$
$$P_{no\ load} = P_{elec} \tag{15}$$
$$P_{load} = P_{elec} + P_{mech} \tag{16}$$
$$P_{mech} = P_{load} - P_{no\ load} \tag{17}$$

Where I is the current across the electrodes and V is the voltage across the electrodes. With these equations, the power used by the unloaded (no magnetic field present) circuit could be measured and then subtracted from the measured electric power to the loaded circuit.

For a rough estimate of the force on a piece of fluid, all effects except the Lorentz force can be discarded, giving

$$|\overrightarrow{F_L}| \approx |I\overrightarrow{w} \times \overrightarrow{B}| = IwB = \frac{V}{R}wB = VwB\frac{h\,w}{\rho_s\ell} = \frac{VBw^2h}{\rho_s\ell} \qquad (18)$$

With B as the magnitude of the magnetic field. This will allow for "sanity checks" on initial

results.

Looking next at efficiency, the total current is:

$$I = \frac{V}{R} - \frac{E_I\,w}{R} \qquad (19)$$

By defining efficiency η as what is produced over what is put in:

$$\eta \equiv \frac{E_I\,w}{V} = \frac{B|\overrightarrow{v}|w}{V} \qquad (20)$$

Then, using (8), (19) can be rewritten as:

$$I = \frac{1-\eta}{\eta}\frac{Bvh\ell}{\rho_s} \qquad (21)$$

From (12), the Lorentz force $|\overrightarrow{F_L}| = I\ell B$ becomes:

$$F_L = \frac{1-\eta}{\eta}\frac{B^2vwh\ell}{\rho_s} \qquad (22)$$

The mechanical power is the Lorentz force times the velocity, giving:

$$P_{mech} = F_L\,v = \frac{1-\eta}{\eta}\frac{B^2v^2wh\ell}{\rho_s} \qquad (23)$$

With the electrical power equaling the current times the voltage:

$$P_{elec} = V\,I = \frac{1-\eta}{\eta}\frac{VBvh\ell}{\rho_s} \qquad (24)$$

Dividing the electric power by the mechanical power returns (20), meaning the definition of η

still holds. Substituting (20) into (23), we get

$$P_{mech} = \frac{\eta(1-\eta)}{\rho_s} \frac{V^2 h\ell}{w} \tag{25}$$

Finding the maximum of this by taking its derivative with respect to η and setting it to zero returns:

$$\frac{\partial P_{mech}}{\partial \eta} = \frac{V^2 h\ell}{\rho_s w}(1 - 2\eta) = 0 \tag{26}$$

Which is true when $\eta = \frac{1}{2}$, meaning maximum efficiency for this type of drive is 50%. These equations will give a point of reference to compare to experimental findings.

Fluid Velocity

The velocity v is the average distance the water traveled, d, divided by the time it took, t:

$$v = \frac{d}{t} \tag{27}$$

Experiments

Computer Model

The first part of the experiment was to form a mathematical model of the thruster given certain boundary conditions. Initially, C++ was to be used, though a Wolfram Mathematica model was a better fit due to more experience with the latter. The overall format of the code involved solving the force per unit volume differential equation (11) for velocity, then varying the water salinity to see the effect on steady-state velocity.

The equations and the code make a few assumptions. The first approximation is that water is incompressible. This is a good approximation as pressure changes due to compression are negligible. The next approximations are that forces from viscosity and gravity are negligible, and that all water molecules collisions are significantly stronger than electrostatic repulsion effects. Since the study takes place at low speeds and low resistivities, relativistic and Hall effect contributions can be ignored. This allowed for an estimate of the final speed of the drive, akin to a DC motor's free spin.

Electrical Power vs. Mechanical Power

The second stage of the project involved a small-scale prototype. The intent behind this was to observe the Lorentz force acting on the water and draw conclusions from it that could be scaled up to a final version. The sizing of the small-scale prototype tube was 5.5 cm by 5.4 cm by 20.8 cm, with currents of approximately 3 amps and average perpendicular magnetic field strength of 0.16 tesla. The main takeaways from the initial prototype were the voltage tests and the salinity by mass resistivity verification. These gave a baseline for fits to ohmic or non-ohmic resistance graphs, and allowed for an estimated load resistance of the fluid during thruster operation.

For the scaled-up prototype, the tube was kept the same dimensions with both the magnetic field strength and current across the electrodes being increased. Larger permanent magnets were used, with the average field strength mapped at about 0.70 tesla by using a gaussmeter held parallel with the ground. Current was sourced from a power source instead of batteries, with a value of about 5 amps. The fluid velocity was initially approximated in this case by observing electrolysis bubbles in the salt water at the thruster output. A video with a stopwatch recorded bubble position in relation to a ruler and hence a rough velocity was found.

This was refined with ink added to the input of the thruster. Velocity was then quantified in the same way.

Like the small-scale prototype, the voltage and current into the system were measured. Firstly, a voltage and current sweep was done with no magnetic field. This effectively measured the resistance of the salt water across the electrodes measured. Next the magnets were mounted, and another voltage and current sweep was done. By subtracting these two values the power that went to moving the water was calculated. From here the efficiency (20) was defined and could be then optimized. This process was undertaken for four percent, seven percent, and ten percent salinity by mass, with the resulting points plotted as current versus voltage (Figure 6).
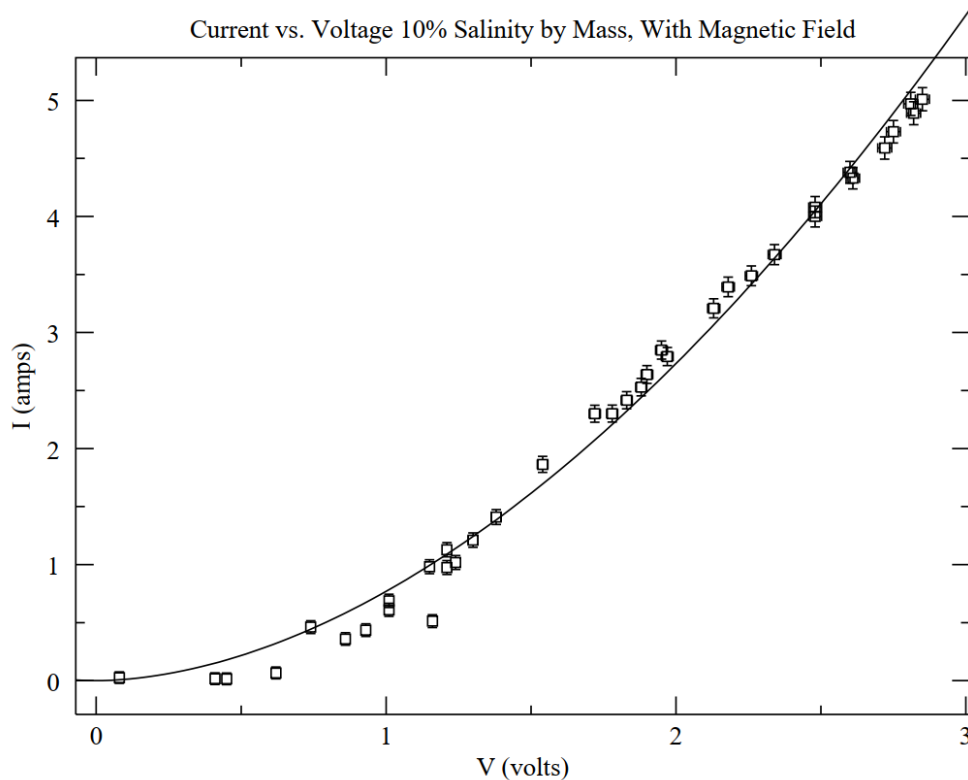

Figure 6: Current vs. voltage of the drive (power law fit).

A certain "threshold" voltage appears in the graphs. While a power law fit approximates the distribution, eliminating values below the x-intercept gave a fit with a much lower reduced

chi-squared. This effect was seen in each of the three different salinities, with the range of x-intercepts varying from 0.66V to 0.96V. While initially puzzling, further research showed this is due to the "electrode potential" of electrodes in water. The standard electrode potential for water is 0.83 V, meaning a certain voltage must be overcome to move current through water. This was an interesting finding in analysis and could be an experiment on its own.

Pressure Differential

The next part of the experiment was to observe a pressure differential. The drive creates a pressure increase to move the fluid. By having a vertical tube of water connected to the thruster, a height difference due to pressure change could be observed (Figure 7). Using this method, the "torque" of the drive could be measured at different salinities, giving a quantification of the force per area (pressure) output.
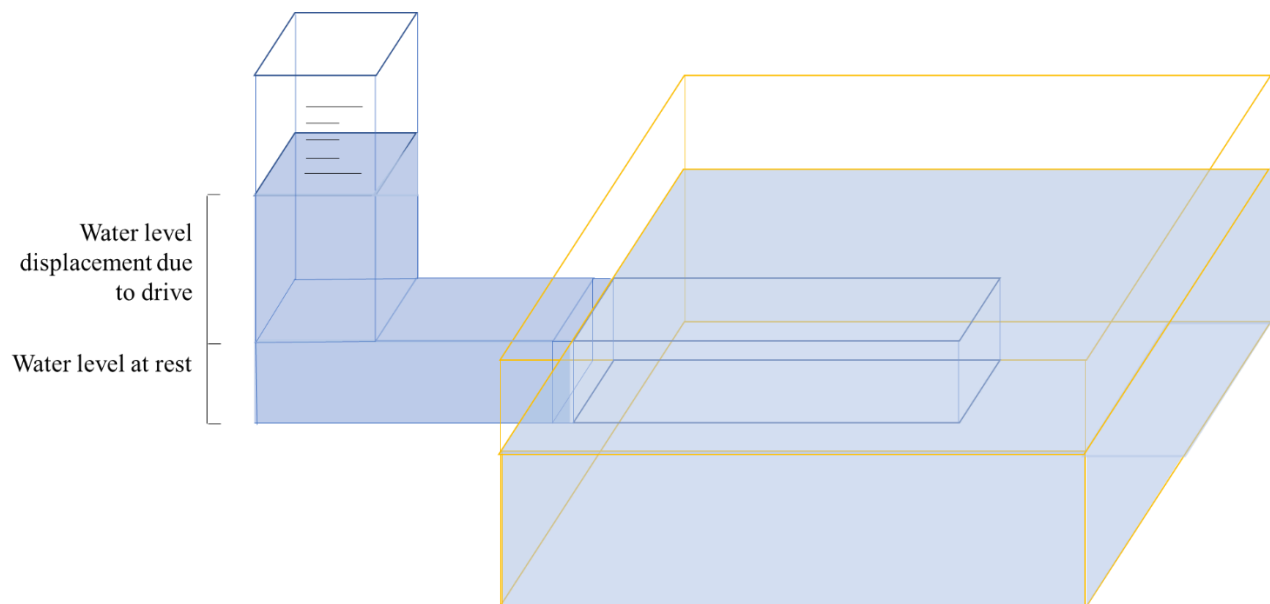

Figure 7: Exaggerated pressure differential.

Fluid Velocity

Fluid velocity was measured with ink droplets and video analysis. A drop of ink was entered into the tube intake and recorded against a ruler to give distance over time. Multiple runs were taken, and a syringe was used for precise ink placement. Video analysis gave many data points allowing for an average velocity varying by salinity to be measured. These were then compared to the Mathematica velocity solution for quantification.

Optimization

Optimization was to take place on two fronts: tube length, and electrolyte (salt in this case) resistivity. Due to the price of permanent magnets, tube length optimization was determined to be outside the scope of the project and resistivity optimization was focused on instead. Using the same camera setup, different water salinities by mass were subject to these three experiments and then recorded, with differences noted after predictions were made. The main goal in optimization was to maximize the efficiency (20) of the drive.

Analysis

Computer Model and Fluid Velocity

The computer model analysis gave a velocity reference point to compare the ink flow data with. By solving (11) in Wolfram Mathematica for velocity as a function of time and distance through the tube, a one-dimensional approximation to the flow was made. The solution to the differential equation leveled off quickly to a different steady-state velocity depending on water salinity (Figure 8).
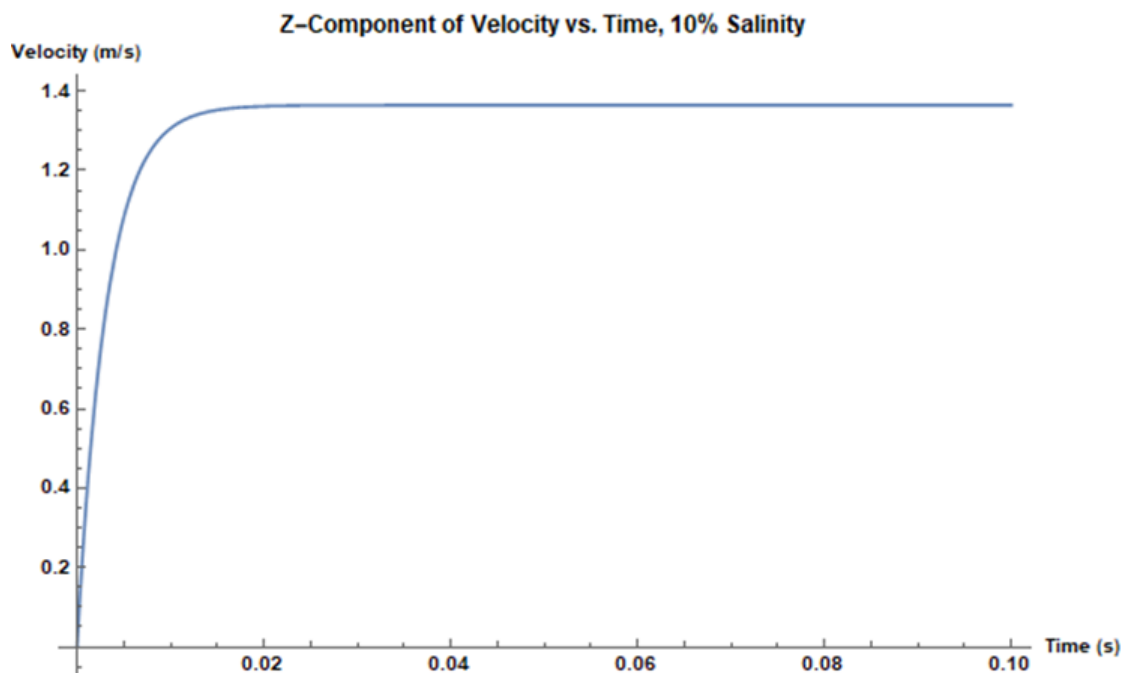

Figure 8: Wolfram Mathematica velocity prediction plot.

These were compared to experimental values (Table 2). Error values are low for the predicted values based on constant magnetic field and ideal power source assumptions.

Salinity by mass	Measured velocity (m/s)	Predicted velocity (m/s)
4%	0.87 ± 0.10	0.99 ± 0.01
7%	0.90 ± 0.10	1.21 ± 0.01
10%	1.12 ± 0.10	1.36 ± 0.01

Table 2: Table of measured and predicted velocity values.

The predicted velocities were higher than the measured velocities for every salinity, and no measurement was within uncertainty. This may be due to the mathematical model assuming no losses except for those due to the induced electric field. Friction, eddy currents, irregularities in the magnitude of the magnetic field, losses due to heat, and losses due to chemical changes were not accounted for. Various improvements to the rough model could increase precision and accuracy but predicted values within approximately twenty-five percent of measured values provided a point of reference.

Pressure Differential

In a no flow, steady-state scenario, the force the drive generates can be quantified by measuring the vertical displacement the water level experiences. Using video analysis, the height difference was measured from rest to equilibrium with the force then calculated (Table 3). The measured value was compared to the rough estimate equation (18).

Salinity by mass	Measured water differential (mm)	Force on fluid particle, measured (N)	Force on fluid particle, estimate (N)
4%	0.5 ± 0.3	0.009 ± 0.009	0.020 ± 0.008
7%	1.0 ± 0.3	0.019 ± 0.009	0.026 ± 0.009
10%	1.4 ± 0.3	0.028 ± 0.009	0.040 ± 0.012

Table 3: Force on fluid particle by salinity.

Sources of error in the height differential experiment were dimensional measurement inaccuracies (though a standard PVC elbow joint used provided a precise inside diameter value), video analysis errors, and no true steady-state equilibrium being reached due to drive fluctuations (mostly due to non-constant magnetic field).

Electrical Power vs. Mechanical Power

The initial analysis of this experiment was done was on the small-scale prototype, with the voltage and current measured to find the loaded and unloaded resistance of the water and verify it against resistivity versus water salinity tables. The results were the on same order of known values, so the method was used again on the large-scale prototype with an improved circuit.

Equation (20) only holds for identical currents. Because of this, electrical power in and mechanical power out data points had to be at the same current to be subtracted. Two values were compared to the measured value: one from the linear fit of the respective graph, and one

from equation (23) using the measured velocity from the ink velocity experiment. Although uncertainty was large, mechanical power generally decreased as salinity increased (Table 4).

Salinity by mass	Current (amps)	Mech. Power measured (W)	Mech. Power expected from fits (W)	Mech. Power expected from (23) (W)
4%	5.02 ± 0.10	0.79 ± 1.15	2.83 ± 0.79	0.75 ± 0.65
7%	5.02 ± 0.10	0.93 ± 0.87	0.88 ± 0.21	0.98 ± 0.64
10%	5.02 ± 0.10	0.37 ± 0.80	0.55 ± 0.18	0.47 ± 0.57

Table 4: Mechanical power measured vs. expected by salinity.

As expected, resistance decreased as salinity increased. This was found as the inverse of the slope for a current versus voltage graph. Similarly, increases in salinity had diminishing returns as predicted by Table 1. Some sources of error were corroding electrode connections, chemical changes in the water, digital multimeter uncertainties, and fluctuating resistances (again due to non-constant magnetic field).

Optimization and Trends

Some of the key assumptions in my analysis are that strong collisions occur between fluid particles, resistivity is small, speeds are non-relativistic, flow scales are not smaller than water particle diameter, changes in the resistivity due to the induced electric field are negligible, and heat increases from fluid friction are negligible. These all stem from an ideal magnetohydrodynamic system using water as the medium. Another source of error was the change in resistance due to temperature. To control for this, water temperature was monitored,

and the drive ran only for short periods of time to avoid operating at non-standard temperatures. The benefit of defining efficiency as a ratio means that some systematic error is eliminated.

The efficiency of Yamato-1 was roughly twenty percent (Sasakawa). The peak efficiency of this drive at similar salinity was $3.7 \pm 0.1\%$, though this is heavily influenced by the drive's small scale and the lack of additional fluid drag due to watercraft area. Additional salinities had higher efficiencies, as expected (Table 5). Expected efficiencies were calculated by dividing the mechanical power out by the electrical power in at the same currents (20).

Salinity by mass	Measured efficiency	Expected efficiency
4%	0.037 ± 0.010	0.046 ± 0.001
7%	0.060 ± 0.010	0.081 ± 0.002
10%	0.084 ± 0.012	0.088 ± 0.002

Table 5: Drive efficiency vs. salinity by mass.

Some trends observed were the decrease of mechanical power with increased salinity, higher speeds at higher salinities, and lower resistance as drive run time went on. The lower salinities seem to provide more "torque," while the higher salinities provided more speed. The resistance also seemed slightly lower after the drive had been running for some time. The recirculated water may have undergone a chemical change making it more conductive. This would also skew the efficiency and mechanical power output as they are resistance dependent. All these observations were also taken at low currents; these trends might not hold once hundreds or thousands of amps are sent through the water.

Conclusion

In this experiment, a magnetohydrodynamic drive was optimized through electrolyte manipulation. The drive was characterized through velocity, mechanical power, and force measurements. Overall efficiency was calculated, and errors were discussed.

The accuracy of assumptions is a central part of this experiment. The main assumptions come from ideal magnetohydrodynamics: strong collisions between fluid particles, small resistivities, and macroscale flow observations. Collisions between molecules is the same as saying water is incompressible. It is what drives bulk motion of the fluid, and without this assumption, the density of water would change with time, meaning that equation (4) would add complexity to the final differential equation (11). This factor is why water is often studied in the field of fluid dynamics. Small resistivities are present in seawater and approximations of seawater, so the second assumption is valid. Finally, charge carries (water molecules and salt ions) are smaller than the flow scale being observed.

Other assumptions stem from electricity and magnetism. These say that eddy currents, Hall effects, and resistivity contributions from the induced electric field are negligible. For a small-scale experiment such as these, they are unlikely to contribute meaningfully; but, as in the Yamato ship (Sasakawa), these do add up once currents reach thousands of amps. Gravity, tube friction, and viscosity forces are also neglected. Gravity does not affect flow in the one-dimensional approximation, but as pressure gradients and bulk flow are added, this would have a noticeable effect.

The efficiencies measured here were not close to the roughly twenty percent efficiency of the Yamato-1 in seawater-like conditions (Sasakawa). However, this drive used permanent

magnets as opposed to helium supercooled electromagnets, meaning the total electrical power used was much higher and hence efficiency is likely much lower.

The next steps in this project is to model the flow more completely in three dimensions, create a more constant magnetic field, find other parameters to optimize like tube length, study the electrochemical processes associated with recirculated water having lower resistance and electrode potential, and finally finding new ways to limit losses. From this, a better understanding of inefficiency contributions could be reached. Optimization of the drive could then take a more targeted approach. Electromagnets weren't investigated in this project, though they could be implemented to increase the strength and constancy of the magnetic field. A more in-depth computer simulation would lend spatial optimization: ideal tube size and length could be found in a three-dimensional model. Finally, electrolysis and standard electrode potential could be better understood to reduce its effect on fluid flow and to be conducive to more accurate results. Currently, MHD propulsion seems stuck where it was in the 1990s, "…unable to vie in efficiency with ships using conventional modes of propulsion. Further R&D efforts are required to put the innovative propulsion system to practical use" (Sasakawa). Perhaps further study in this area could lead to MHD ships in the future.

Acknowledgements

Bibliography

Choudhary, Vikrant S, et al. "Performance Analyses of MHD Thruster." Performance-Analyses-

of-MHD-Thruster-Using-CAE-Tools.docx, www.ijser.org/paper/Performance-analyses-

of-MHD-Thruster-using-CAE-tools.html.

Crain, E. R. Crain's Petrophysical Handbook - Water Resistivity And Water Salinity Methods,

spec2000.net/14-swrw.htm.

Gilbert, J. B., and T. F. Lin. "Studies of MHD Propulsion for Underwater Vehicles and Seawater

Conductivity Enhancement." Applied Research Laboratory, Department of the Navy

Office of Naval Research, Feb. 1991.

Sasakawa, Yohei, et al. "The Superconducting MHD-Propelled Ship Yamato-1." NASA

Technical Reports Server, NASA, 1991,

ntrs.nasa.gov/archive/nasa/casi.ntrs.nasa.gov/19960000249.pdf.

WAPP+: Web-Based Analysis Program for Physics,

www.physics.csbsju.edu/stats/WAPP2.html.